Int. J. Electrochem. Sci., 11 **(2016)** 175 - 188

International Journal of
ELECTROCHEMICAL
SCIENCE
www.electrochemsci.org

UV Tuning of Cadmium Telluride Quantum Dots (CdTe QDs) – Assessed by Spectroscopy and Electrochemistry

Lukas Nejdl[1,2], *Lukas Richtera*[1,3], *Kledi Xhaxhiu*[4], *Renata Kensova*[1,3], *Jiri Kudr*[1,3], *Branislav Ruttkay-Nedecky*[1,3], *Jindrich Kynicky*[1,2], *Dorota Wawrzak*[5], *Vojtech Adam*[1,3], *Rene Kizek*[1,3], *Pavel Kopel*[1,3,*]

[1]Central European Institute of Technology, Brno University of Technology, Technicka 3058/10, CZ-616 00 Brno, Czech Republic - European Union
[2]Department of Geology and Pedology, Mendel University in Brno, Zemedelska 1, CZ-613 00 Brno, Czech Republic - European Union
[3]Department of Chemistry and Biochemistry, Mendel University in Brno, Zemedelska 1, CZ-613 00 Brno, Czech Republic - European Union
[4]Department of Chemistry, Faculty of Natural Sciences, University of Tirana, Blv. Zog I, No.2/1, 1001, Tirana, Albania
[5]Institute of Chemistry, Environmental Protection and Biotechnology, Jan Dlugosz University of Czestochowa, Armii Krajowej 13/15, PL-42201 Czestochowa, Poland
[*]E-mail: paulko@centrum.cz

Received: 23 September 2015 / *Accepted:* 8 October 2015 / *Published:* 1 December 2015

In this work, the electrochemical analysis (potentiometric stripping analysis – PSA, cyclic voltammetry – CV) and evaluation of fluorescence properties of cadmium telluride quantum dots (CdTe QDs) covered by mercaptosuccinic acid (MSA) were performed. Using CV it was found that average value of ΔE of QDs is lower than 0.059 V and I is in direct correlation with square root of scan rates, therefore it can be assumed that this system represents rather reversible than quasi-reversible process. Further, it was found that nearly 1.4 electrons are exchanged in both cases, which corresponded with expected two-electron transfer. Fluorescence analysis showed that UV radiation (254 and 312 nm) significantly changes fluorescence properties of CdTe QDs in time 0 – 60 min. It was found that after 5 min of UV irradiation (λ = 312 nm) the fluorescence intensity increased by 37% and at λ = 254 nm the increase in fluorescence intensity was even higher, by 45% (compared to the control without irradiation). UV radiation also caused a shift in the emission maximum of CdTe QDs in range 2 – 70 nm. This work opens up new ways for tuning the optical properties of QDs.

Keywords: Cyclic voltammetry; Fluorescence analysis; Nanoparticles; Potentiometric stripping analysis; Quantum dots; Synthesis; UV radiation; UV tuning;

1. INTRODUCTION

Nanotechnology is one of the most advanced disciplines. One of the main areas of nanotechnology is the synthesis and characterization of various types of nanoparticles for a wide spectrum of applications [1-3]. Entry into the nano world has opened up new possibilities for the use of fluorescent nanocrystals better known as quantum dots (QDs) and utilization of their unique properties [4]. QDs were first reported by Alexey Ekimov in 1981 in a glass matrix and then in colloidal solutions by Louis E. Brus in 1985 [5]. QDs were one of the first nanoparticles to be integrated within the biological sciences that were used for imaging or tracking macromolecules/cells in cell/tissue [6]. The popularity of QDs is mainly due to a wide variety of different types of preparation and functionalization of their surface [7-10]. QDs retain part of the properties of the material, from which they are made, but also take over the new properties that are related to their size (size-dependent optical absorption and emission) [11]. For biological applications, the most frequently used are CdSe, CdSe/ZnS or CdTe, CdTe/CdS nanocrystals [12-19]. The particles are generally made of hundreds or thousands of atoms mainly of group II and VI elements (CdSe and CdTe QDs) or group III and V elements (InP and InAs QDs) [20].

The most popular methods for QDs synthesis are organometallic synthesis, aqueous route (low-temperature reaction) and biosynthesis [6]. An interesting complement to these methods can be post-synthesis of QDs by exposure to the UV radiation. In this way, the surface of QDs can be activated and optical properties of QDs can be controlled (tuned). The ability of UV light to change the conformation of complexes was studied in our previous work [21]. It has been demonstrated that UV radiation activates fluorescence of zinc(II) complexes. The light-induced control of various type of emulsions (oil or water continuous medium) stabilized by an appropriate combination of two polyelectrolyte surfactants was described [22]. Furthermore, a number of photocatalytically active nanoparticles has been reviewed e.g. TiO_2 nanorods [23], ZnO nanoparticles [24] and others [25,26]. Corrosion of the outer sphere of nanoparticles caused by photooxidation leading to toxic ion release, formation of reactive oxygen species (ROS) or induction of genotoxic stress was reported [27-29]. Yin et al. showed that the toxic effect of PbSe QDs under UV irradiation is caused by release of Pb(II) and generation of ROS, inducing DNA damage [30]. Photocatalytic technique can be used for metals removal or transformation of free ions to the less toxic species or their deposition on the semiconductor catalyst surface for metals recovery [31]. In our experiments, we have focused on the electrochemical study of CdTe QDs with mercaptosuccinic acid on surface and subsequent fluorescent analysis of QDs exposed to UV radiation at two wavelengths $\lambda = 254$ and $\lambda = 312$ nm in time intervals 0 – 60 minutes. For electrochemical investigation of QDs CV and PSA were chosen. By studying the data obtained from the CV reversibility of electrode reactions, number of electrons transferred, the kinetics of the individual reaction steps, stability of the resulting intermediates, adsorption and desorption on the electrode material from the electrode can be determined. Because of its simplicity and economy, PSA is considered a very useful electrochemical technique for metal traces determination [32-37]. This highly sensitive microanalytical technique was used e.g. for heavy metal low concentration determination in soil or in herbal drugs [38-40]. Traces of soluble lead in glassware were determined by this method too [41]. Another application of PSA method is the determination of metals in human teeth and dental materials [42,43]. The simplest PSA modification uses dissolved oxygen as the oxidizing agent. Thus, the contamination risk arising from the application of some externally added oxidizing agents [44-46]is reduced. In this article, a significant ability of UV light to alter the fluorescence properties of CdTe QDs was described, which can be used to improve the quantum yield of QDs, or adjusting (tuning) the emission maxima for the particular application.

2. EXPERIMENTAL PART

2.1 Chemicals

Working solutions like buffers and standard solutions were prepared daily by diluting the stock solutions. Standards and other chemicals were purchased from Sigma-Aldrich (St. Louis, MO, USA) in ACS purity unless noted otherwise.

2.2 Preparation of CdTe QDs

CdTe QDs were prepared according to the following protocol. Briefly, 10 mL of cadmium(II) acetate (5.34 $mg\cdot mL^{-1}$) and 1.0 mL of mercaptosuccinic acid solution (60.0 $mg\cdot mL^{-1}$) were mixed with 76.0 mL of deionized water on a magnetic stirrer. Subsequently 1.8 mL of ammonia (1.0 M) solution was added to the reaction mixture. Then 1.5 mL of sodium tellurite (4.43 $mg\cdot mL^{-1}$) was also added under continuous stirring and later 40 mg of sodium borohydride was added. The solution was stirred for around 2 h until the bubble formation finished and subsequently the volume of the solution was diluted up to 100 mL with deionized water. Volume of 2.0 mL of prepared solution was taken in a small glass vessel and heated at 100 °C, 300 W for 20 min (ramping time 10 min) under microwave irradiation (Multiwave 3000, Anton-Paar GmbH, Graz, Austria) and finally the prepared CdTe QDs were stored in the dark at 4 °C.

2.3 Determination of cadmium by atomic absorption spectrometry

Cadmium concentration was determined using 280Z Agilent Technologies atomic absorption spectrometer (Agilent, Santa Clara, CA, USA) with electrothermal atomization. Cadmium ultrasensitive hollow cathode lamp (Agilent) was used as the radiation source (lamp current 4 mA). The spectrometer was operated at 228.8 nm resonance line with spectral bandwidth of 0.5 nm. The sample (10 µL) was injected into the graphite cuvette. The flow of argon inert gas was 300 $mL\cdot min^{-1}$. Zeeman background correction was used with field strength 0.8 T. Cadmium was determined in the presence of palladium chemical modifier.

2.4 Electrochemical measurement (PSA and CV)

Determination of Cd(II) and CdTe QDs by PSA and CV was performed with 797 VA Computrace instrument (Metrohm, Switzerland), using a standard cell with three electrodes. A hanging mercury drop electrode (HMDE) with a drop area of 0.4 mm^2 was employed as the working electrode. An Ag/AgCl/3M KCl electrode was used as the reference and carbon electrode served as auxiliary. For data processing 797 VA Computrace software by Metrohm CH was employed. The analyzed samples were deoxygenated prior to measurements by purging with argon (99.999%). Determination of Cd(II) and CdTe QDs was performed with acetate buffer (0.2 M CH_3COONa and CH_3COOH, pH 5) as a supporting electrolyte. The supporting electrolyte was exchanged after each analysis. Volume of sample 15 µL, total volume of measurement cell 2 mL (15 µL of sample + 1985 µL acetate buffer). The parameters of the measurement by PSA were as follows: initial potential of -0.70 V, end potential -0.25 V, number of cycles 1, deoxygenating with argon 60 s, potential limit -0.25 V, maximal time 360 s (pre-treatment used parameters: cleaning potential -0.70 V, cleaning time 60 s, deposition potential -0.70 V, deposition time 600 s, equilibration time 15 s). Measurements were carried out at 25 ± 1 °C. CV was carried with same electrochemical apparatus as in the case PSA was used. The parameters of the measurement were as follows: initial potential of -0.80 V, first vertex potential -0.20 V, second vertex potential -0.80 V, deoxygenating with argon 90 s, deposition 0 s, voltage step 5 mV, scan rate 6.25 - 400 mV·s^{-1}, deposition potential -0.80 V.

2.5 Fluorescence analysis

Fluorescence was acquired by multifunctional microplate reader Tecan Infinite 200 M PRO (TECAN, Switzerland). Wavelength 360 nm was used as an excitation radiation and the fluorescence scan was measured within the range from 400 to 850 nm per 2-nm steps. The detector gain was set to 65. The samples were placed in UV-transparent 96 well microplate with flat bottom by CoStar (Corning, USA). To each well 50 µL of sample was placed. All measurements were performed at 25 °C controlled by Tecan Infinite 200 PRO (TECAN, Switzerland). The QDs were exposed to UV radiation at 254 and 312 nm using transilluminator (Vilber Lourmat, Marne-la-Vallee Cedex, France). The sample area is 20 × 20 cm illuminated by 6 UV emitting tubes with power of 15 W each. The intensity of UV radiation incoming to the UV-transparent 96-well microplate was recorded by instrument for the determination of optical power (PM100D, sensor SV120VC, Thorlabs Inc., Newton, NJ, USA). Based on these measurements the intensity of incoming UV energy into the sample was determined: $E = 3.12$ mW ($\lambda = 312$ nm) and $E = 4.18$ mW ($\lambda = 254$ nm).

2 .6 Particle size and zeta-potential analysis

Zetasizer MALVERN, Malvern Instruments Ltd. Worcestershire WR14 1XZ, United Kingdom was used.

2.6.1 Zeta potential assessment

The particle size measurements were performed considering the same refraction index and absorption coefficient as described in particle size measurements. Furthermore, the measuring parameters such as, temperature and viscosity were the same as in particle size measurements (see below). Calculations considered the diminishing of particles concentration based Smoluchowsky model, with a $F(\kappa a)$ of 1.50 and an equilibrating time of 120 s. For the measurements, a disposable cell DTS1070 was employed. In each case, the measurement duration depended on the number of runs, which varied between 20 and 40. The measurements were carried out in triplicates and were performed under the automatic setting of attenuation and voltage selection.

2.6.2 Particle size assessment (dynamic light scattering)

The particle size measurements were performed considering a refraction index of the dispersive phase of 3.00 and 1.33 for the dispersive environment. The absorption coefficient in both cases was 10^{-3}. The measuring temperature was set at a constant value of 25 °C, while the viscosity was 0.8872 cP. For each measurement, disposable cuvettes type ZEN 0040, were used, containing 40 µL of sample. The equilibration time was 120 s, at a measurement angle of 173° backscatter. All measurements were triplicate ($p < 0.05$) and the data was expressed as the average value.

3. RESULTS AND DISCUSSION

3.1 Electrochemical behavior of Cd(II) and CdTe QDs

QDs and cadmium standard were studied and characterized using CV and PSA. CV is popular for its relative simplicity and its high information content. It is used most often as a diagnostic tool for elucidating electrode mechanisms. The advantage of PSA technique is purported to be its lower susceptibility to interferences from adsorption of organic molecules on the electrode surface (deposition step is identical to that in the anodic stripping techniques) [47]. First, stock solutions of Cd(II) and CdTe QDs were united according to total concentration of Cd(II) by atomic absorption spectrometry (AAS) and electrochemically analyzed.

3.1.1 Cyclic voltammetry of Cd(II) and CdTe QDs

Cyclic voltammograms of 3 µM Cd(II) solution at different values of scan rate (6.25 – 400 $\mathrm{mV \cdot s^{-1}}$) were recorded, Fig. 1 A. Further, the plotted I_{pc} (cathodic current) and I_{pa} (anodic current) on scan rate (Fig. 1 B) and scan rate root $v^{1/2}$, Fig. 1 C. In the case of CdTe QDs was followed in the same way. Cyclic voltammograms of 3 µM CdTe QDs solution at different values of scan rate (6.25 – 400 $\mathrm{mV \cdot s^{-1}}$) were recorded (Fig. 1 B) and subsequently I_{pc} (cathodic current) and I_{pa} (anodic current) on scan rate (Fig. 1 E) and scan rate root $v^{1/2}$ (Fig. 1 E) were evaluated. Observed values are shown in the tables, Tab. 1 A Cd(II) and B CdTe QDs. In all cases, linear dependence was observed. Given that the average value ΔE is less than 0.059 V, while the I value is directly proportional to the square root of scan rate, it can be assumed that the investigated redox events Cd(II) and CdTe QDs taking place at the electrode are rather reversible than quasireversible. The number of exchanged electrons at redox events Cd(II) and CdTe QDs electrode is according to the relation ($\Delta E_p = E_{pa} - E_{pc} = 2.303\,RT/nF$) equal in both cases and reaches approximately 1.4, reflecting the anticipated transfer of two electrons. The dependence of the CV analytical signal of Cd(II) and CdTe QDs scan rate root gave the following equations:

I_{pc} (nA) = 9.6 $v^{1/2}$ (mV$^{1/2}$·s$^{-1/2}$), R^2 = 0.9982, n = 3 Cd(II)
I_{pa} (nA) = -6.3 $v^{1/2}$ (mV$^{1/2}$·s$^{-1/2}$), R^2 = 0.9348, n = 3 Cd(II)
I_{pc} (nA) = 8.2 $v^{1/2}$ (mV$^{1/2}$·s$^{-1/2}$), R^2 = 0.9967, n = 3 CdTe QDs
I_{pa} (nA) = -5.8 $v^{1/2}$ (mV$^{1/2}$·s$^{-1/2}$), R^2 = 0.9373, n = 3 CdTe QDs

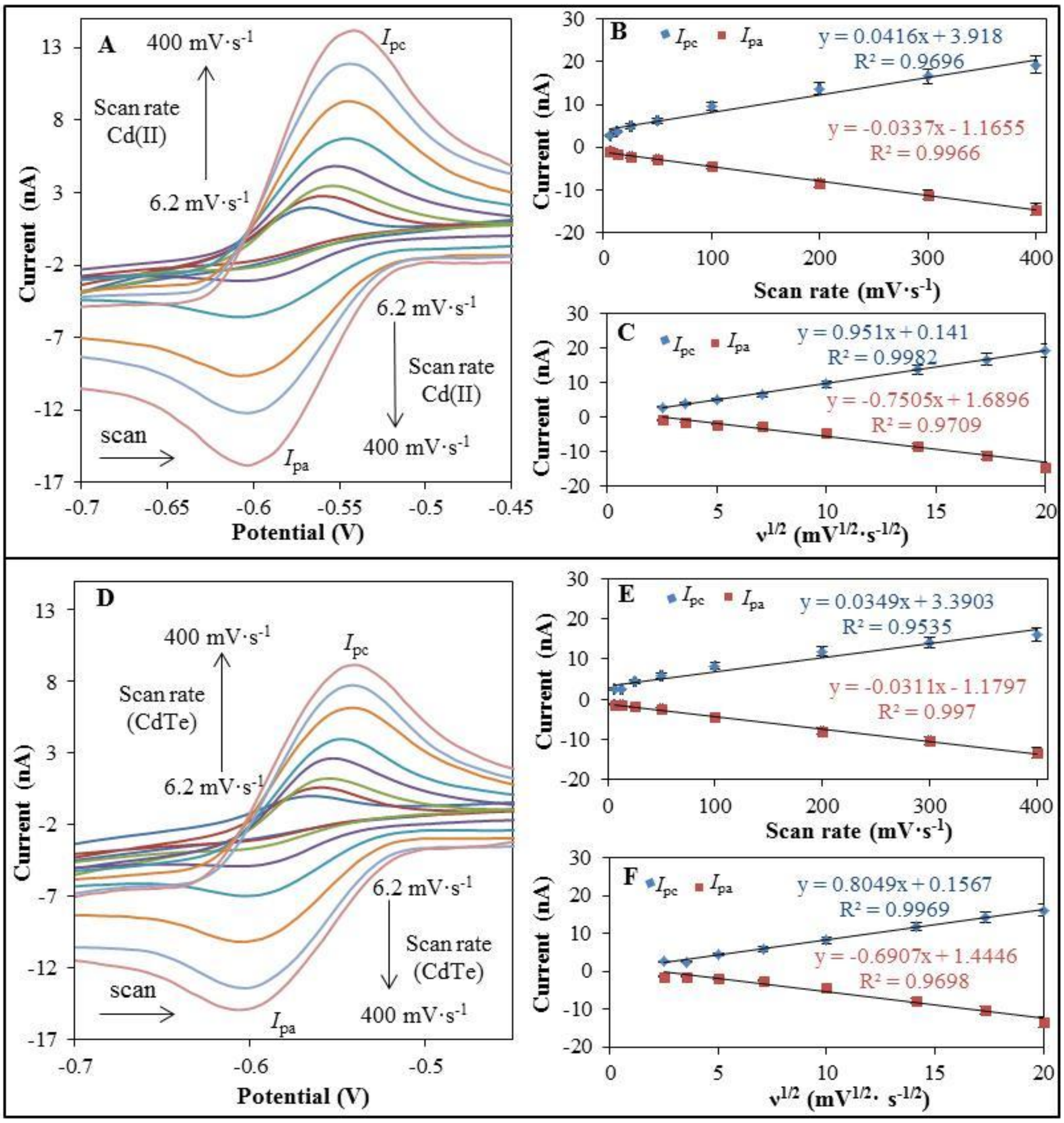

Figure 1. (**A**) Cyclic voltammograms of Cd(II) measured at different values of scan rate (6.25 – 400 mV·s^{-1}). Dependence (Cd(II)) of I_{pc} and I_{pa} on scan rates (**B**) and square root of scan rates $v^{1/2}$ (**C**). (**D**) Cyclic voltammograms of CdTe measured at different values of scan rate (6.25 – 400 mV·s^{-1}). Dependence (CdTe) of I_{pc} and I_{pa} on scan rates (**E**) and square root of scan rates $v^{1/2}$ (**F**). For all electrochemical experiments 3 µM Cd(II) and 3 µM CdTe solutions were used.

Table 1. Electrochemical parameters based on cyclic voltammograms for (**A**) 3 µM Cd(II) and (**B**) 3 µM CdTe QDs.

A **Cd(II)**

Sc. Rate [mV·s^{-1}]	$v^{1/2}$ [V$^{1/2}$·s$^{-1/2}$]	E_{pc} [V]	I_{pc} [nA]	E_{pa} [V]	I_{pa} [nA]	ΔE [V]	I_{pc}/I_{pa}
6.25	2.50	-0.57	2.8	-0.61	-1.0	0.04	-2.8
12.5	3.54	-0.57	3.7	-0.62	-1.6	0.06	-2.30
25	5.00	-0.56	4.9	-0.60	-2.2	0.05	-2.20
50	7.07	-0.56	6.3	-0.60	-2.8	0.04	-2.23
100	10.00	-0.56	9.5	-0.59	-4.5	0.04	-2.11
200	14.14	-0.55	13.7	-0.60	-8.5	0.04	-1.61
300	17.32	-0.55	16.6	-0.60	-11.1	0.05	-1.50
400	20.00	-0.56	19.3	-0.59	-14.5	0.04	-1.33

B **CdTe QDs**

Sc. Rate [mV·s^{-1}]	$v^{1/2}$ [V$^{1/2}$·s$^{-1/2}$]	E_{pc} [V]	I_{pc} [nA]	E_{pa} [V]	I_{pa} [nA]	ΔE [V]	I_{pc}/I_{pa}
6.25	2.50	-0.57	2.5	-0.62	-1.4	0.05	-1.78
12.5	3.54	-0.57	2.4	-0.62	-1.4	0.05	-1.71
25	5.00	-0.56	4.4	-0.60	-1.9	0.04	-2.31
50	7.07	-0.56	5.8	-0.60	-2.5	0.04	-2.32
100	10.00	-0.56	8.2	-0.59	-4.5	0.04	-1.82
200	14.14	-0.55	11.8	-0.59	-7.9	0.04	-1.49
300	17.32	-0.55	14.1	-0.60	-10.4	0.04	-1.35
400	20.00	-0.56	16.1	-0.59	-13.4	0.04	-1.20

3.1.2 Potentiometric stripping analysis (PSA) of Cd(II) and CdTe QDs

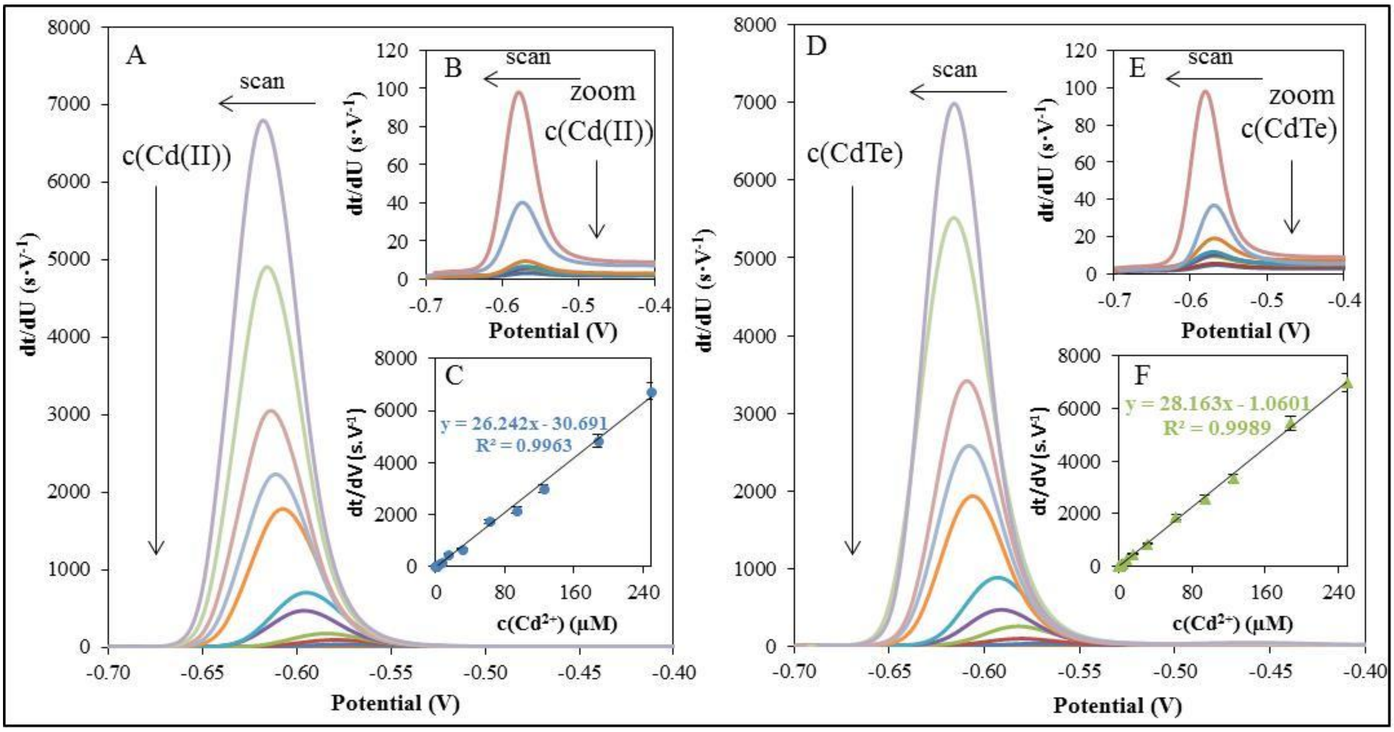

Figure 2. (**A**) PSA voltammograms of Cd(II) and (**B**) detail of voltammograms (zoom). (**C**) The calibration curve of Cd(II) in the linear range 0.03 – 240 µM. (**D**) PSA voltammograms of CdTe QDs and **E)** detail of voltammograms (zoom). (**F**) The calibration curve of CdTe QDs in the same range as Cd(II).

Electrochemical responses of different concentrations of Cd(II) and CdTe QDs were compared using PSA. This method enables more precise analysis of samples compared to differential pulse or square wave voltammetry, due to the lower influence of various interferents on the measurement [47]. At first, the linearity and reproducibility of the PSA analytical signal of Cd(II) was checked. The analytical signal was found to be a linear function of the Cd(II) concentrations within the concentration range of 0.03 – 240 μM (Fig. 2 A and zoom B). The dependence of the PSA analytical signal on the mass concentration of Cd(II) in sample gave the following equation:

$dt/dV\ (s\cdot V^{-1}) = 26.24\ c_{Cd(II)}\ (\mu M) - 30.69$, $R^2 = 0.9963$, n = 3 (Fig. 2 C).

In the case of CdTe QDs, measurement was performed in the same way. Fig. 2 D shows the voltammograms of CdTe QDs and zoom, Fig. 2 E. The dependence of the PSA analytical signal on the mass concentration of CdTe QDs in sample gave the following equation:

$dt/dV\ (s\cdot V^{-1}) = 2.816\cdot 10^{1}\ c_{Cd(II)}\ (\mu M) - 10.060$, $R^2 = 0.9989$, n = 3 (Fig. 2 F)

According to the high values of the coefficients of determination ($R^2 = 0.9963$ and 0.9989 for Cd(II) and CdTe QDs, respectively), it can be concluded that there was a very good linearity of the PSA analytical signals within the examined concentration ranges of cadmium. This method confirmed the results from CV, this means that the electrochemical behavior of Cd(II) and CdTe QDs is similar.

3.2 UV interaction with CdTe QDs (color tuning)

Fluorescence spectroscopy was employed for monitoring the interaction of UV radiation with CdTe QDs in time. Emission spectra in the range of 400 – 800 nm with excitation wavelength of 360 nm at temperature 25 °C were obtained. Conditions mentioned above were used for all measurements. CdTe QDs were exposed to UV radiation ($\lambda = 312$ and $\lambda = 254$ nm) for 5 minutes in the transilluminator and emission spectra of samples were measured in five-minute time intervals up to 60 minutes . The samples were placed in UV-transparent 96 well microplate with flat bottom. After irradiation, the fluorescence properties of QDs (fluorescence intensity and emission maximum) were monitored immediately. This process was repeated twelve times to observe the UV dose dependency. First, transilluminator was set on 312 nm. After that, samples (50 μL of 1 mM QDs in UV-transparent 96 well microplate) were inserted into the transilluminator.

It was found that after 5 min of UV irradiation ($\lambda = 312$ nm) the fluorescence intensity increased by 37% (compared to the control without irradiation) and the color changed from green to light green, Fig. 3 A. Another five-minute irradiation caused an increase in fluorescence intensity further by 9% and the color turned to yellow-green. Another ten-minute irradiation caused an increase in fluorescence intensity by approximately 1% and the color turned yellow. Each subsequent irradiation caused a decrease in fluorescence intensity of QDs by 10%. The last two UV exposures in time of 55 and 60 minutes caused a color change to bright orange (in 55 minutes) and orange (in 60 minutes). Further, the dependence of the UV radiation on the change of the emission maximum of QDs was observed, Fig. 3 B. In control QDs (without irradiation), the emission maximum at $\lambda_{em} = 522$ nm was found. Five minutes of UV irradiation ($\lambda = 312$ nm) caused a shift in emission maximum for 4 nm. Another five-minute exposure to UV radiation caused a shift in emission maximum for another 8 nm. Another ten-minute irradiation caused a shift by 14 nm and another ten-minute irradiation by 16 nm. After 60 minutes of UV irradiation of QDs emission maximum of $\lambda_{em} = 570$ nm was achieved. Second, transilluminator was set on 254 nm and the same measurements were carried out as in the previous case.

It was found that after 5 min of UV irradiation ($\lambda = 254$ nm) the fluorescence intensity increased by 45% (compared to the control without irradiation) and the color changed from green to light green, Fig. 3 C. Another five-minute irradiation caused a decrease in fluorescence intensity by 12% and the color was yellow. Each additional radiation exposure caused a slight decrease (approximately by 3.5%) of QDs fluorescence intensity. UV exposure in time of 35, 40, 45 and 50 minutes caused a color change to bright orange (in 35 minutes) and orange (in 40, 45, 50 minutes). The last two UV exposures in time of 55 and 60 minutes caused a color change to bright red. The shift in emission maximum of QDs depending on the UV irradiation length had a similar trend as in the previous case, Fig. 3 D. Five minutes of UV irradiation ($\lambda = 254$ nm) caused a shift in emission maximum for 4 nm. Another five-minute exposure to UV radiation caused a shift in emission maximum for another 8 nm. Another ten-minute irradiation caused shift by 36 nm and another ten-minute irradiation by 18 nm. After 60 minutes of UV irradiation of QDs emission maximum $\lambda_{em} = 592$ nm was achieved.

The two general existent strategies (control size) of nanocrystal preparations are an organometallic synthesis based on the high-temperature thermolysis of the precursors [48,49] and the synthesis in an aqueous medium [50,51].

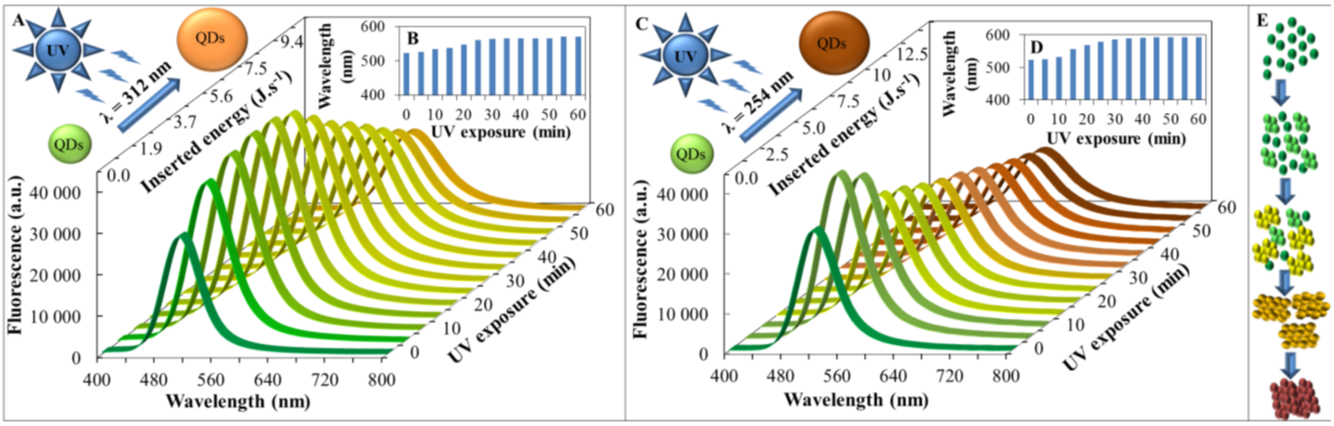

Figure 3. (**A**) The effect of UV radiation ($\lambda = 312$ nm, E = 3.12 mW) on the change in fluorescence properties of 1 mM QDs and (**B**) emission maximum of QDs during exposure to UV radiation (0 – 60 min). (**C**) The effect of UV radiation ($\lambda = 254$ nm, E = 4.18 mW) on the change in fluorescence properties of QDs and (**D**) emission maximum of QDs during exposure to UV radiation 0 – 60 min. (**E**) Schematic representation of the effect of UV radiation on the increase in size of CdTe QDs.

The size and the emission color of QDs can be tuned by varying the reflux time [52], growth temperatures [53] or pH change [54]. The photoluminescence of the graphene QDs can be due to charge transfers between functional groups of graphene QDs [55]. The technique presented in this paper can be used for the easy, inexpensive and fast synthesis or the post-synthesis (tuning) of CdTe QDs stabilized by MSA. Probable mechanism is that the UV light causes an increase in size or aggregation of CdTe QDs (Fig. 3 E), which lead to a change in their optical properties. Increase in size of the CdTe QDs was determined by dynamic light scattering (DLS) as we show below in the next section. Guo-Yu Lan et al. described the photo-assisted synthesis of highly fluorescent ZnSe (S) QDs in aqueous solution stabilized by MSA [56]. They observed an increase in the intensity of fluorescence of ZnSe (S) QDs after UV irradiation, which is consistent with our work. Photoetching of CdTe nanocrystals was applied to thiol-capped CdTe QDs to control their fluorescence wavelength by Uematsu et al. [57].

3.3 Particle size, zeta-potential and CV analysis after UV irradiation

The interaction of CdTe QDs with UV radiation was subsequently monitored using size analysis, zeta-potential and cyclic voltammetry. CdTe QDs (1 mM) were pipetted into 2 mL Eppendorf tubes and then placed into a UV transilluminator ($\lambda = 312$ or 254 nm) for 0, 10, 20, 30, 40, 50 and 60 min of irradiation. At each step of size or zeta potential determination, DLS measurements and photo documentation were performed. After irradiation of sample, an analysis was started immediately. First, CdTe QDs were irradiated under UV with $\lambda = 312$ nm. Fig. 4 A show the real photo (under UV light) of CdTe QDs after 0 – 60 min exposure of UV irradiation ($\lambda = 312$ nm). As discussed in the previous chapter, the change in emission of fluorescence is closely associated with resizing of CdTe QDs. The size increase and stable zeta potential (average -33 mV) of CdTe QDs after each UV irradiation was monitored using zetasizer, see Fig. 4 B. Resizing of CdSe QDs corresponds to the change in fluorescence, which is consistent with the literature [58,59]. The zeta potential of the solid-liquid interface is a fundamental parameter in models of electrical double layers and their associated properties. The value of the zeta potential indicates the stability of the colloidal system. Particles with zeta potential more positive than +30 mV or more negative than -30 mV are considered as stable [60]. Second, CdTe QDs were irradiated under UV with $\lambda = 254$ nm. Fig. 4 C shows the real photo (under UV light) of CdTe QDs after 0 – 60 min exposure of UV irradiation ($\lambda = 312$ nm). The size increase and stable zeta potential (average -33 mV) of CdTe QDs after each UV irradiation was similar as in the previous case, Fig. 4 D. With DLS measurements was confirmed that the UV radiation can be a useful instrument for the preparation of stable and different sized CdTe QDs. Parallel electrochemical analysis (CV) of CdTe QDs was carried out at the same time. After each irradiation in time (0, 10, 20, 30, 40, 50 and 60 minutes) an aliquot (15 μL) was removed and analyzed by CV. 15 mL of CdTe QDs were diluted with 0.2 M acetate buffer pH 5 in total 1 mL and immediately analyzed. Electrochemical response of CdTe QDs at a scan rate of 50 $mV\cdot s^{-1}$ was monitored. In both cases, faintly growing electrochemical signals were observed, Fig. 4 E and F. The observed signals increase was insignificant in the context of a 4% RSD, but stability of potential was unchanged (approximately -0.56 V). In this way was shown that increasing the size of CdTe QDs is not proportional to the value of the electrochemical signal, which is consistent with the results from the first chapter.

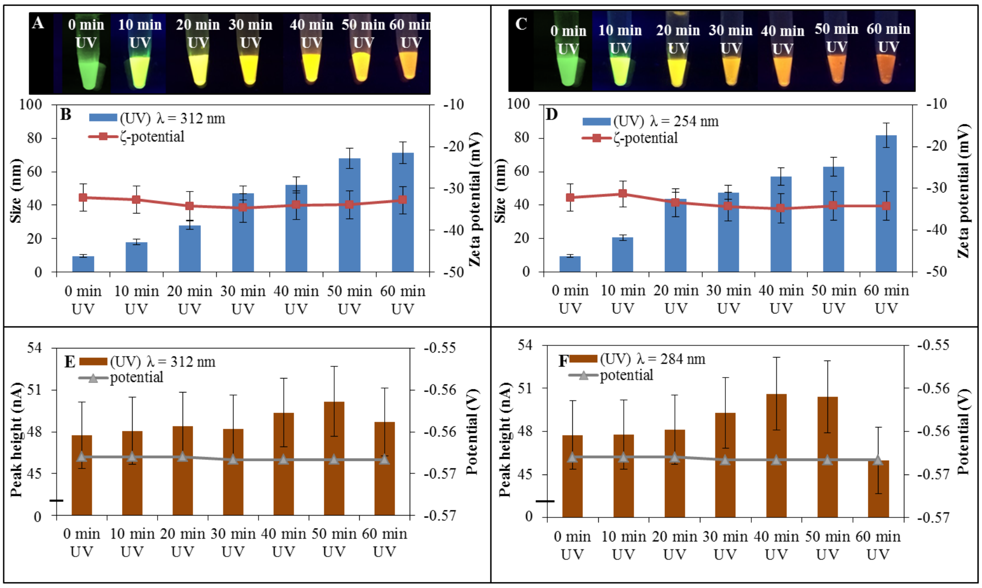

Figure 4. (**A**) Real photo of CdTe QDs (under UV light) after UV exposure (λ = 312 nm) in time 0 - 60 min. (B) The average size and zeta potential of CdTe QDs after UV irradiation (λ = 312 nm) in time 0 – 60 min. C) Real photo of CdTe QDs (under UV light) after UV exposure (λ = 254 nm) in time 0 – 60 min. D) The average size and zeta potential of CdTe QDs after UV irradiation (λ = 254 nm) in time 0 – 60 min. Electrochemical signals (CV) of 3 µM CdTe QDs after UV irradiation E) λ = 312 nm and F) λ = 312 nm in time 0 – 60 min at initial potential of -0.80 V, first vertex potential -0.20 V, second vertex potential -0.80 V, deoxygenating with argon 90 s, deposition 0 s, voltage step 5 mV, scan rate 50 mV·s^{-1}, deposition potential -0.80 V.

The zeta potential, or potential at the solid-liquid interface (more precise definitions are to follow), is a fundamental parameter in models of electrical double layers and their associated properties

4. CONCLUSIONS

In this work, CdTe QDs covered by MSA were studied using electrochemistry and spectroscopy. The electrochemical characterization by CV and PSA offered the monitoring of oxidation and reduction behavior of QDs and subsequently, the number of electrons exchanged between working electrode and sample solution was calculated. It was found out that the processes on the working electrode are rather reversible than quasi-reversible and nearly 1.4 electrons are exchanged, which corresponded with expected two electron transfer.

Using fluorescence spectroscopy, a significant relationship between CdTe QDs and UV radiation (λ = 312 and 254 nm) was found. It was observed that exposure to UV light changes the optical characteristics (radiation intensity and emission) of CdTe QDs. The increase of the fluorescence intensity at the beginning of the UV light illumination was caused probably by formation of new QDs from precursors present in the solution. On the other hand, the emission maximum shift (green to red) was caused by aggregation of the QDs. Finally, the electrochemical signal of CdTe QDs of different sizes was observed by CV and it was shown that increasing the size of CdTe QDs is not proportional to the value of the electrochemical signal.

In general, the method of UV-illumination synthesis (or post-synthesis) described in this paper can be effectively employed for rapid and inexpensive tuning of QDs optical properties for the particular application.

In this work, CdTe QDs covered by MSA were studied using electrochemistry and spectroscopy. Using fluorescence spectroscopy, a significant relationship between QDs and UV radiation was found. It was observed that exposure to UV light changes the optical characteristics (radiation intensity and emission) of QDs. In this way QDs can be controlled and tuned for better quantum yield, or to adapt the emission spectrum for the particular application. In further work, various types of QDs will be studied (modified by UV radiation) and mechanism responsible for fluorescence changes induced by UV radiation will be elucidated.

ACKNOWLEDGEMENTS

Financial support from UGP ID: 1912015 and MENDELU IGA project IP 05 2015 is are highly acknowledged

Conflict Of Interest

The authors have declared no conflict of interest.

References

1. O. C. Farokhzad and R. Langer, *ACS Nano* 3 (2009) 16.
2. Q. Chaudhry, M. Scotter, J. Blackburn, B. Ross, A. Boxall, L. Castle, R. Aitken and R. Watkins, *Food Addit. Contam. Part A-Chem*. 25 (2008) 241.
3. X. Wang, L. L. Yang, Z. Chen and D. M. Shin, *CA-Cancer J. Clin.* 58 (2008) 97.
4. M. Bruchez, M. Moronne, P. Gin, S. Weiss and A. P. Alivisatos, *Science* 281 (1998) 2013.
5. A. I. Ekimov and A. A. Onushchenko, *Sov Phys Semicond* 16 (1982) 775.
6. S. M. Farkhani and A. Valizadeh, *IET Nanobiotechnol*. 8 (2014) 59.
7. Z. Heger, J. Zitka, N. Cernei, S. Krizkova, M. Sztalmachova, P. Kopel, M. Masarik, P. Hodek, O. Zitka, V. Adam and R. Kizek, *Electrophoresis* 36 (2015) 1256.
8. K. Grieve, P. Mulvaney and F. Grieser, Curr. Opin. Colloid Interface Sci. 5 (2000) 168.
9. R. M. Penner, *Accounts Chem. Res*. 33 (2000) 78.
10. Z. Heger, N. Cernei, S. Krizkova, M. Masarik, P. Kopel, P. Hodek, O. Zitka, V. Adam and R. Kizek, *Sci Rep* 5 (2015)
11. D. J. Norris and M. G. Bawendi, *Phys. Rev. B* 53 (1996) 16338.
12. A. Samanta, Z. T. Deng and Y. Liu, *Langmuir* 28 (2012) 8205.
13. W. C. W. Chan, D. J. Maxwell, X. H. Gao, R. E. Bailey, M. Y. Han and S. M. Nie, *Curr. Opin. Biotechnol*. 13 (2002) 40.
14. S. M. Reimann and M. Manninen, *Rev. Mod. Phys.* 74 (2002) 1283.
15. M. Ryvolova, J. Chomoucka, J. Drbohlavova, P. Kopel, P. Babula, D. Hynek, V. Adam, T. Eckschlager, J. Hubalek, M. Stiborova, J. Kaiser and R. Kizek, *Sensors* 12 (2012) 14792.
16. K. Tmejova, D. Hynek, P. Kopel, S. Krizkova, I. Blazkova, L. Trnkova, V. Adam and R. Kizek, *Colloid Surf. B-Biointerfaces* 117 (2014) 534.
17. L. Hlavata, I. Striesova, T. Ignat, J. Blaskovisova, B. Ruttkay-Nedecky, P. Kopel, V. Adam, R. Kizek and J. Labuda, *Microchim. Acta* 182 (2015) 1715.

18. A. Moulick, I. Blazkova, V. Milosavljevic, Z. Fohlerova, J. Hubalek, P. Kopel, M. Vaculovicova, V. Adam and R. Kizek, *Photochem. Photobiol.* 91 (2015) 417.
19. Z. Heger, N. Cernei, I. Blazkova, P. Kopel, M. Masarik, O. Zitka, V. Adam and R. Kizek, *Chromatographia* 77 (2014) 1415.
20. X. H. Gao, L. L. Yang, J. A. Petros, F. F. Marshal, J. W. Simons and S. M. Nie, *Curr. Opin. Biotechnol.* 16 (2005) 63.
21. L. Nejdl, L. Richtera, D. Wawrzak, V. Milosavljevic, P. Kopel, J. Kudr, B. Ruttkay-Nedecky, V. Adam and R. Kizek, *Int. J. Electrochem. Sci*. 10 (2015) 1696.
22. I. Porcar, P. Perrin and C. Tribet, *Langmui*r 17 (2001) 6905.
23. T. A. Kandiel, R. Dillert, A. Feldhoff and D. W. Bahnemann, *J. Phys. Chem. C* 114 (2010) 4909.
24. X. J. Liu, L. K. Pan, Q. F. Zhao, T. Lv, G. Zhu, T. Q. Chen, T. Lu, Z. Sun and C. Q. Sun, *Chem. Eng. J.* 183 (2012) 238.
25. H. Schmidt, M. Akarsu, T. S. Muller, K. Moh, G. Schafer, D. J. Strauss and M. Naumann, *Res. Chem. Intermed.* 31 (2005) 535.
26. X. B. Chen, S. H. Shen, L. J. Guo and S. S. Mao, *Chem. Rev*. 110 (2010) 6503.
27. J. Aldana, Y. A. Wang and X. G. Peng, *J. Am. Chem. Soc.* 123 (2001) 8844.
28. A. C. S. Samia, X. B. Chen and C. Burda, *J. Am. Chem. Soc.* 125 (2003) 15736.
29. A. O. Choi, S. E. Brown, M. Szyf and D. Maysinger, *J. Mol. Med.* 86 (2008) 291.
30. C. X. Yin, T. Yang, W. Zhang, X. D. Zhou and K. Jiao, *Chin. Chem. Lett*. 21 (2010) 716.
31. M. I. Litter, *Appl. Catal. B-Environ.* 23 (1999) 89.
32. M. B. Arain, T. G. Kazi, M. K. Jamali, N. Jalbani, H. I. Afridi, G. A. Kandhro, R. Ansari and R. A. Sarfraz, *J. Hazard. Mater*. 155 (2008) 216.
33. K. Becker, C. Schulz, S. Kaus, M. Seiwert and B. Seifert, *Int. J. Hyg. Environ. Health*. 206 (2003) 15.
34. M. M. Brzoska and J. Moniuszko-Jakoniuk, Arch. Toxicol. 72 (1998) 63.
35. B. B. Clarke and E. Brennan, *JAPCA J Air Waste Ma* 39 (1989) 1319.
36. Z. Suturovic, S. Kravic, S. Milanovic, A. Durovic and T. Brezo, *Food Chem*. 155 (2014) 120.
37. D. Jagner, Analyst 107 (1982) 593.
38. B. Kaličanin and D. Velimirović, *Cent. Eur. J. Biol.* 8 (2013) 178.
39. B. Kalicanin and D. Velimirovic, *Int. J. Electrochem. Sci.* 7 (2012) 313.
40. B. Kalicanin and D. Velimirovic, *Cent. Eur. J. Biol*. 8 (2013) 178.
41. B. M. Kalicanin, N. J. Marjanovic and Z. J. Suturovic, *J. Serb. Chem. Soc*. 67 (2002) 213.
42. B. M. Kalicanin and R. S. Nikolic, *J. Trace Elem. Med. Biol.* 22 (2008) 93.
43. B. M. Kalicanin, R. S. Nikolic and N. J. Marjanovic, *Anal. Chim. Acta* 525 (2004) 111.
44. I. Gondola and I. Kadar, A*cta Agronomica Hung* 43 (1994) 243.
45. C. A. Grant, W. T. Buckley, L. D. Bailey and F. Selles, *Can. J. Plant Sci.* 78 (1998) 1.
46. E. E. Golia, A. Dimirkou and I. K. Mitsios, *Bull. Environ. Contam. Toxicol.* 80 (2008) 206.
47. R. M. Town, *Electroanalysis* 9 (1997) 407.
48. C. B. Murray, D. J. Norris and M. G. Bawendi, J. Am. Chem. Soc. 115 (1993) 8706.
49. Z. A. Peng and X. G. Peng, *J. Am. Chem. Soc*. 123 (2001) 183.
50. A. L. Rogach, L. Katsikas, A. Kornowski, D. S. Su, A. Eychmuller and H. Weller, Ber. Bunsen-Ges. *Phys. Chem. Chem. Phys.* 100 (1996) 1772.
51. D. V. Talapin, A. L. Rogach, E. V. Shevchenko, A. Kornowski, M. Haase and H. Weller, *J. Am. Chem. Soc.* 124 (2002) 5782.
52. Y. L. Wang, S. Y. Liu and L. Y. Zhou, *Chin. Chem. Lett*. 23 (2012) 359.
53. Y. W. Jun, J. E. Koo and J. Cheon, *Chem. Commun*. (2000) 1243.
54. Y. Zhang, L. Mi, P. N. Wang, J. Ma and J. Y. Chen, *J. Lumines*. 128 (2008) 1948.
55. S. H. Jin, D. H. Kim, G. H. Jun, S. H. Hong and S. Jeon, *ACS Nano* 7 (2013) 1239.
56. G. Y. Lan, Y. W. Lin, Y. F. Huang and H. T. Chang, *J. Mater. Chem.* 17 (2007) 2661.

57. T. Uematsu, H. Kitajima, T. Kohma, T. Torimoto, Y. Tachibana and S. Kuwabata, *Nanotechnology* 20 (2009) 1.
58. N. Manabe, S. Hanada, N. Aoki, Y. Futamura, K. Yamamoto and T. Adschiri, *J. Chem. Eng. Jpn.* 45 (2012) 917.
59. M. Simsikova, M. Antalik, M. Kanuchova and J. Skvarla, *Appl. Surf. Sci*. 282 (2013) 342.,
60. B. J. Kirby and E. F. Hasselbrink, *Electrophoresis,* 25 (2004) 187.